

PACS numbers: 42.55.Rz; 42.60.By; 42.60.Lh
DOI: 10.1070/QE2013v043n03ABEH015064

Calculation of the gain coefficient in cryogenically cooled Yb:YAG disks at high heat generation rates

O.L. Vadimova, I.B. Mukhin, I.I. Kuznetsov, O.V. Palashov, E.A. Perevezentsev, E.A. Khazanov

Abstract. **We have calculated the stored energy and gain coefficient in disk gain elements cooled to cryogenic temperatures. The problem has been solved with allowance for intense heat generation, amplified spontaneous emission and parasitic lasing, without averaging over any spatial coordinate. The numerical simulation results agree well with experimental data, in particular at high heat generation rates. Experimental data and theoretical analysis indicate that composite disk gain elements containing an undoped region can store considerably more energy due to suppression of amplified spontaneous emission and parasitic lasing.**

Keywords: *pulsed laser, disk laser, amplified spontaneous emission, Yb:YAG, cryogenic cooling.*

1. Introduction

The ability to reduce negative thermal effects (such as thermally induced aberrations or reduction in gain cross section), the power scalability of laser systems and the laser damage behaviour of gain elements (GEs) are critical issues in designing high pulse energy, high repetition rate laser systems. One way to resolve these issues is to use Yb:YAG disks cooled to liquid-nitrogen temperature [1, 2]. The ytterbium ion has a small quantum defect (9%) [3] and long inversion lifetime and is free from excited-state absorption [4]. The use of face-cooled (active mirror) disk GEs greatly reduces thermally induced aberrations [5] and allows one to readily scale up laser systems by merely increasing the pump and transmitted beam diameters. Yet another advantage of the disk geometry is that no self-focusing occurs because of the small laser–material interaction length. Cooling to cryogenic temperatures increases the thermal conductivity of Yb:YAG, reduces its thermal expansion coefficient $(1/L)(\mathrm{d}L/\mathrm{d}T)$ and changes its refractive index $(\mathrm{d}n/\mathrm{d}T)$ [6, 7]. Moreover, it improves the lasing performance of the medium: increases its absorption and stimulated-emission cross sections [8] and almost completely depopulates its lower laser level [4], which enables more energy to be stored in the GE.

The key factors that limit the energy stored in disk elements are amplified spontaneous emission (ASE) and parasitic lasing. These effects are particularly strong in the case of disk geometry, with low longitudinal and high transverse gain. The effect of ASE on the small-signal gain coefficient has been the subject of extensive experimental and theoretical studies [9–15]. Most analytical and even numerical calculations have been only approximate.

In a number of studies [9–12], ASE was treated as a modifier of the upper laser level lifetime. In this approach, the temperature dependence and nonuniformity of the population distribution are left out of consideration. Antognini et al. [9] measured the effective upper laser level lifetime as a function of pump power and used the results in their analytical calculations. The lifetime was estimated analytically in Refs [10–12], and Speiser [13] presented an analytical calculation of the ASE flux density with no allowance for the longitudinal nonuniformity of the population distribution. His model took into account back reflection from the faces and reflection loss, with no allowance for temperature changes. Xinghua et al. [14] evaluated ASE using a Monte Carlo method, which requires no approximations, but they did not assess the associated temperature change. Their model took into account back reflection from the disk faces and neglected the reflection loss, and the lateral surface was thought to be absorbing. Albach [15] also evaluated ASE using Monte Carlo simulation. He took into account the nonuniformity of the distribution of the population difference between the laser levels; solved a linear problem for the temperature; and took into account the thermal effects, such as thermal lensing, thermal depolarisation and birefringence; but back reflection was left out of account.

Researchers at the Institute of Applied Physics, Russian Academy of Sciences, are developing a cryogenic 100 ps disk laser with a subjoule energy and repetition rate of 1 kHz [16]. In this paper, we present a numerical model for evaluating the stored energy and small-signal gain in a disk GE. The model takes into account amplified spontaneous emission and parasitic lasing in the GE, the spectral distributions of the gain and absorption cross sections, the highly nonuniform heat generation and nonuniform distributions of material parameters because of the temperature gradient across the GE. In our calculations, no averaging over any coordinate was performed.

2. Calculation of the population inversion in a gain element

Let a pump beam of fixed power P and diameter D be incident on a disk GE of thickness h and diameter d (Fig. 1). The pump beam passes twice through the GE because it reflects from the face having a mirror. The gain element is in thermal

O.L. Vadimova, I.B. Mukhin, I.I. Kuznetsov, O.V. Palashov, E.A. Perevezentsev, E.A. Khazanov Institute of Applied Physics, Russian Academy of Sciences, ul. Ul'yanova 46, 603950 Nizhnii Novgorod, Russia; e-mail: khazanov@appl.sci-nnov.ru, mib_1982@mail.ru, musfex@mail.ru

Received 24 October 2012; revision received 29 November 2012
Kvantovaya Elektronika **43** (3) 201–206 (2013)
Translated by O.M. Tsarev

contact with a copper heatsink through indium solder (Fig. 1). The system is thought to be axisymmetric: the angle of incidence of the pump beam is so small that the azimuthal asymmetry can be neglected. We examine two disk GE configurations: a disk gain element and a composite gain element consisting of an Yb:YAG disk and an undoped YAG crystal fused to the disk (Fig. 1). This structure allows one to improve heat removal from the active medium and reduces the effect of ASE because there is no reflection from the Yb:YAG/YAG interface. The Yb:YAG/YAG composite medium was produced by thermal diffusion bonding [17].

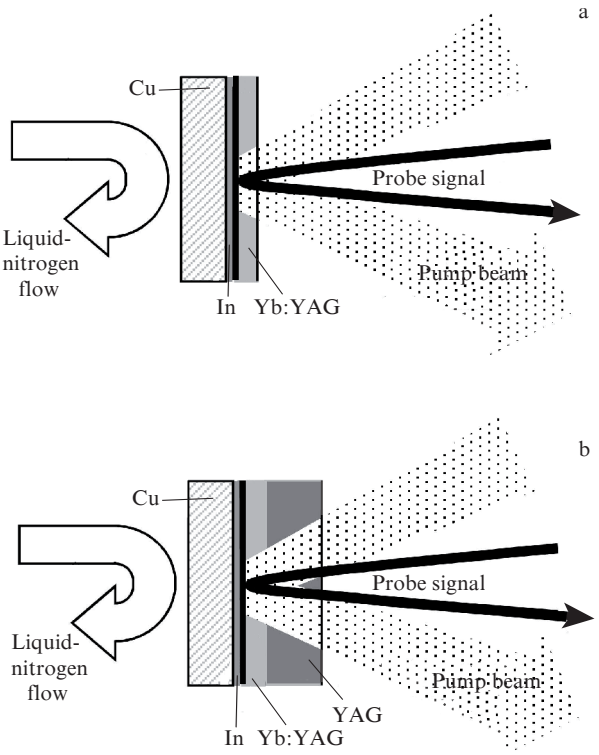

Figure 1. Geometry of Yb:YAG amplifiers with (a) a standard disk GE and (b) a composite GE.

2.1. System of balance equations

To calculate the gain coefficient, one must know the distribution of the population difference between the laser levels. The evolution of this parameter can be described by a system of balance equations for the population of the ytterbium ion levels and the intensity of the incident and reflected pump beams. The energy level structure and parameters of the Yb^{3+} ion are such that there is no absorption from the upper laser level and it has a long lifetime and small quantum defect. The Yb^{3+} ion, however, has a significant drawback: the splitting of its lower and upper laser levels makes it necessary to take into account the population distribution over their sublevels [18]. At room temperature, the splitting leads to a population redistribution between all the sublevels, reducing the population difference and, therefore, the small-signal gain and stored energy. Cooling to liquid-nitrogen temperature reduces kT. The effect of the level splitting also decreases, but we will not neglect it.

To adequately describe the dynamics of the populations in a wide temperature range, we should take into account the temperature dependence of the population distribution over the energy sublevels and temperature-dependent material parameters. The sublevels with populations N_2, N_2' and N_2'' are assumed to instantaneously reach thermodynamic equilibrium with the sublevels with populations N_0, N_1, N_1' and N_1'' in accordance with the Boltzmann distribution. This approximation allows balance equations to be derived for the population of only one level: all the other populations can be expressed through this quantity and the total Yb ion concentration. Given the above, the system of balance equations for the population of the upper laser level (N_2), the incident pump intensity (I_1) and the intensity of the beam reflected from the GE mirror (I_2) has the form

$$\frac{\partial I_1}{\partial z} = \sigma_p(F_1(T)N_2 - F_2(T)N_{tot})I_1, \tag{1}$$

$$\frac{\partial I_2}{\partial z} = -\sigma_p(F_1(T)N_2 - F_2(T)N_{tot})I_2, \tag{2}$$

$$\frac{\partial N_2}{\partial t}F_3(T) = -\frac{I_1 + I_2}{I_{sp}\tau}(F_1(T)N_2 - F_2(T)N_0) - \frac{N_2}{\tau} - \frac{\partial N_2}{\partial t}\bigg|_{ASE}, \tag{3}$$

$$\rho\frac{\partial(a(T)T)}{\partial t} = \mathrm{div}(\kappa(T)\nabla T) + Q(r,t), \tag{4}$$

$$Q(r,t) = \eta\sigma_p(F_1(T)N_2 - F_2(T)N_{tot})(I_1 + I_2), \tag{5}$$

where N_{tot} is the active ion concentration; σ_p is the absorption cross section at the pump wavelength; I_{sp} is the saturation intensity at the pump wavelength; τ is the upper laser level lifetime; $\kappa(T)$ is the thermal conductivity of the GE material; $a(T)$ is its heat capacity; ρ is its density; and $Q(r,T)$ is the heat source, determined by the quantum defect and absorbed pump power. The functions $F_1(T)$, $F_2(T)$ and $F_3(T)$ are determined by the temperature and sublevel energies in accordance with the Boltzmann distribution:

$$\begin{aligned} F_1(T) &= \exp\left(\frac{E_2 - E_2'}{kT}\right) + \left[1 + \exp\left(\frac{E_2 - E_2'}{kT}\right) + \exp\left(\frac{E_2 - E_2''}{kT}\right)\right]\left[1 + \exp\left(\frac{E_0 - E_1}{kT}\right) + \exp\left(\frac{E_0 - E_1'}{kT}\right) + \exp\left(\frac{E_0 - E_1''}{kT}\right)\right]^{-1}, \\ F_2(T) &= \left[1 + \exp\left(\frac{E_0 - E_1}{kT}\right) + \exp\left(\frac{E_0 - E_1'}{kT}\right) + \exp\left(\frac{E_0 - E_1''}{kT}\right)\right]^{-1}, \\ F_3(T) &= 1 + \exp\left(\frac{E_2 - E_2'}{kT}\right) + \exp\left(\frac{E_2 - E_2''}{kT}\right). \end{aligned} \tag{6}$$

Here, E_0, E_1, E_1', E_1'', E_2, E_2' and E_2'' are the energies of the corresponding ytterbium ion sublevels [18]: 0, 565, 612, 785, 10 327, 10 624 and 10 679 cm^{-1}, respectively.

The system is supplemented with a nonlinear heat equation because, at a high thermal load, the temperature dependence of the lasing characteristics of the GE is essential, especially at cryogenic temperatures. The last term in Eqn (3) represents ASE. The particular form of this term is considered below.

2.2. Amplified spontaneous emission

The effect of ASE is taken into account by the last term in (3). It can be written in the form [13]

$$\left(\frac{\partial N_2}{\partial t}\right)\Big|_{\text{ASE}} = \int_{\lambda} \gamma_\lambda \Phi_\lambda \mathrm{d}\lambda, \tag{7}$$

where γ_λ is the linear gain coefficient at wavelength λ and Φ_λ is the ASE flux at frequencies from λ to $\lambda + \mathrm{d}\lambda$. The ASE flux should be integrated with respect to wavelength using the known luminescence spectrum and gain cross section (measured by Mukhin et al. [19]). The ASE flux at wavelength λ can be found as follows [13]:

$$\Phi_\lambda(\hat{\boldsymbol{s}}) = \int \mathrm{d}\Omega \frac{\beta_\lambda}{\tau} \int_0^{s_{\max}} N_2(\boldsymbol{s}) \exp\left(\int_0^{s} \gamma_\lambda(\hat{\boldsymbol{s}}, \tilde{\boldsymbol{s}})\mathrm{d}\tilde{\boldsymbol{s}}\right)\mathrm{d}\boldsymbol{s},$$

$$\int \beta_\gamma \mathrm{d}\lambda = 1, \tag{8}$$

where β_λ is the spectral distribution of the spontaneous emission intensity; $\mathrm{d}\Omega$ is a solid angle element; $\hat{\boldsymbol{s}}$ is the radius vector of the point for which the ASE flux is sought; $\boldsymbol{s}$ is the variable radius vector in the integration over the GE; and $\tilde{\boldsymbol{s}}$ is the radius vector characterising the amplified emission direction.

The integration limit $s_{\max}$ depends on the GE configuration (disk or composite GE). In the case of the disk (with allowance for the back reflection from the disk faces but with no allowance for the reflection from the lateral surface, which is thought to be perfectly absorbing), this parameter is given by [13]

$$s_{\max} = \frac{\sqrt{R^2 - \rho^2 \sin^2\varphi} - \rho\cos\varphi}{\sin\theta}, \tag{9}$$

where R is the GE radius; ρ is the radial distance from the centre of the GE to the point for which the ASE flux is sought; and the angles θ and φ are defined in Fig. 2.

When the ASE intensity in a composite GE is calculated, reflection is though to occur only from the bottom face, i.e. $s_{\max}$ takes a different value. The top face of the GE is not perfectly reflective, so the amplified spontaneous emission can leave the GE through this surface. Its reflectivity was measured as a function of the angle of incidence and was used in ASE intensity calculation.

Spontaneous emission can be scattered from the lateral GE surface back to the pumped region, where it is then further amplified. This process leads to radial ASE intensity oscillations and limits subsequent growth of the stored energy. The parasitic lasing threshold was estimated from the condition that the product of the probability of scattering into the pumped region with the radial spontaneous emission gain should exceed unity. We assumed that the total internal reflection angle was only determined by the refractive index of YAG (Yb^{3+} doping had no effect on its refractive index) and that, on the lateral surface, the light was scattered through the 4π solid angle with equal probability. The gain was estimated using averaging over the longitudinal coordinate of the GE.

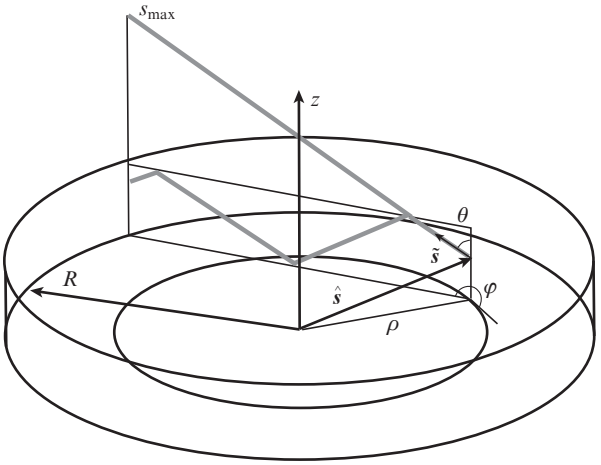

Figure 2. Local coordinate system and determination of the integration limits for a disk in ASE calculation.

2.3. Numerical simulation

To compute the small-signal gain and stored energy in an Yb:YAG disk GE, we designed a program code based on spatial finite differences. Note that it involves no averaging over any spatial coordinate, which allows us to use a numerical model for any cylindrical GE.

In the first step, the incident and reflected pump intensities are evaluated using Eqns (1) and (2). The population difference distribution at the initial instant is thought to be uniform and to correspond to thermal equilibrium, and the temperature of the system is set equal to the ambient temperature. Next, Eqn (3) is used to compute the change in population difference over one time step using the ASE computed in the preceding step. For the new population difference distribution, the heat sources, ASE flux distribution, stored energy and small-signal gain are computed, along with the temperature change over one time step. The program then verifies whether the parasitic lasing condition is met. If so, nonuniform distributions of GE parameters are recomputed using the new temperature distribution. Next, a transition to the next time step occurs.

The temperature is computed for a system of coaxial cylindrical bodies of the same diameter: a copper heatsink, gain element and undoped YAG in the case of the composite GE. At a high thermal load, the problem of heat conduction is nonlinear because of the nonuniform temperature distribution. The calculation takes into account the temperature dependences of the lasing and thermo-optical characteristics of the GE: the upper laser level lifetime, spectra of the stimulated emission and absorption cross sections [20], thermal conductivity [19] and heat capacity [21] of Yb:YAG. Temperature-dependent gain and luminescence spectra were reported by Mukhin et al. [20]. The upper laser level lifetime

is a strong function of the quality of the material, so this lifetime was measured for each sample.

The ASE flux is computed as follows: A local spherical coordinate system is introduced at each point of the computational mesh (Fig. 2). With such a coordinate system, the integral in the expression for the amplified spontaneous emission flux has no singularity, but it adds complexity to the integration limit. Next, Eqn (8) is used to compute the ASE flux arriving at a given point $\hat{s}$ of the GE in a given direction and the result is integrated over all directions. In addition, the ASE flux is summed over wavelengths using measured gain and luminescence spectra [21].

3. Experimental investigation of an Yb:YAG disk GE

To verify simulation results, we carried out a series of experiments in which the gain coefficient in different GEs was measured under various pumping conditions. We studied disk and composite GEs with an Yb:YAG disk 0.06 cm in thickness and 1 cm in diameter. A dielectric mirror was deposited on one face of the samples, and an antireflection dielectric coating, on the other (Fig. 1). The GEs were pumped by a beam with a nonuniform intensity profile, constant average power and effective radius r. We used two pump modes: pulsed, with a pulse duration of 2 ms and repetition rate of 200 Hz, and continuous. In the former mode, one can measure energy deposition dynamics and check simulation results for low heat generation rates, where heating of the GE can be neglected. The latter mode can be used to check simulation results for high heat generation rates. Since some of the pump light left the GE, in what follows we deal only with the absorbed pump power. The small-signal gain was measured using weak light with a centre wavelength of 1029.3 nm and linewidth of 0.8 nm, which passed through the centre of the pumped region of the GE and was amplified.

The maximum gain in the cross section of the disk GE measured as a function of pump energy is shown in Fig. 3a. The measurements were made at different pump beam diameters. The numerical simulation results are seen to agree well with the experimental data. Starting at some energy, the gain stops increasing. Numerical calculation indicates that, at this energy, parasitic lasing occurs, i.e. the estimated parasitic lasing threshold agrees with experimental data.

Vinokurov [22] derived a relation between the volume-averaged gain coefficient with allowance for ASE (γ) and that with no allowance for ASE (γ_0) for a geometry in which the population inversion zone has the form of a sphere of diameter D:

$$\gamma_0 D = 3\left\{\left[1 + e^{\gamma D}(\gamma D - 1)\right]\frac{1}{(\gamma D)^2} - \frac{1}{2}\right\}. \qquad (10)$$

According to his results, ASE has very similar effects on the population inversion in a cylinder and sphere with identical volumes of the inversion zone. Thus, the effect of ASE can be evaluated for almost any GE geometry using the rather simple relation (10). At a uniform pump intensity profile, the present simulation results and the results obtained using Eqn (10) differ very little (Fig. 3a) up to the pump energy at which parasitic lasing begins. At the same time, at nonuniform pump intensity and population inversion profiles, Eqn (10) slightly overestimates the stored energy (Fig. 3b).

Figure 4a shows the small-signal gain as a function of pump energy for the composite and disk GEs at a pump beam

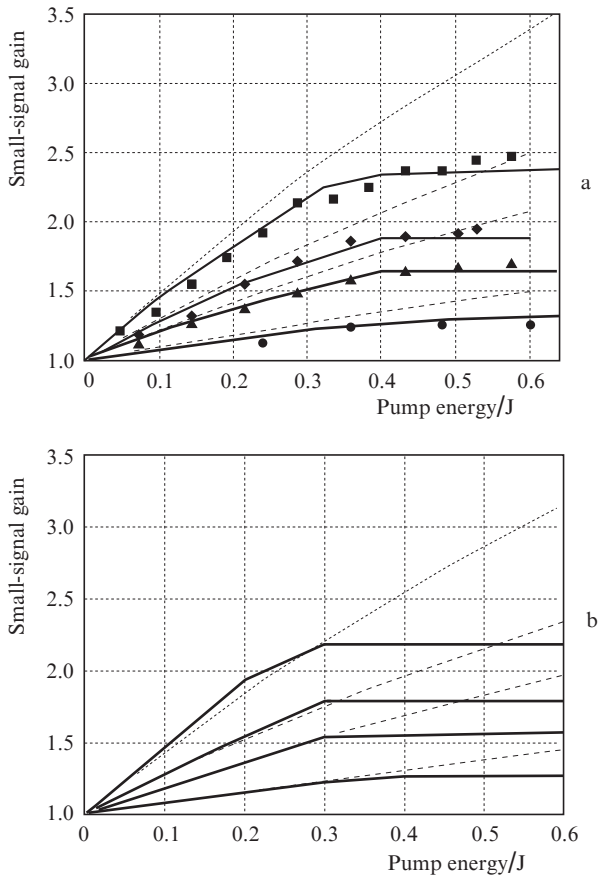

Figure 3. (a) Maximum small-signal gain in the cross section of a GE vs. pump energy at pump beam diameters of 2.7 (■), 3.4 (♦), 4.0 (▲) and 6.0 (●) mm [the solid lines represent simulation results and the dashed lines represent estimates using (10)]. (b) Analogous data for a uniform population distribution in the pumped region at the same pump beam diameters as in panel (a) [the dashed lines represent calculation using Eqn (10) and the solid lines represent results obtained in the model presented in this study].

diameter of 4 mm. In the composite GE, the small-signal gain is considerably higher and, hence, more energy is stored. The reason for this is that spontaneous emission does not experience multiple reflection from the GE faces to the pumped region. This leads as well to a large increase in parasitic lasing threshold. In particular, Fig. 4a demonstrates that, at an absorbed pump energy of 388 mJ, the energy stored in the composite GE reaches 87 mJ, whereas only 63 mJ can be stored in the disk under similar conditions. We measured a time-dependent gain during a pump pulse in the composite GE at an absorbed pump energy of 388 mJ. The calculated time-dependent gain coefficient is in excellent agreement with experimental data (Fig. 4b).

A particularly important point is to check numerical simulation results for high thermal loads. Under cw pumping, the small-signal gain was measured in both the composite and disk GEs. The numerical simulation results agree with the experimental data (Fig. 5) for both GE configurations. Note that, at high heat generation rates, the difference in small-signal gain between the two GEs is rather small. Heating reduces the gain cross section, but, as a consequence, the effect of ASE also decreases, so the gain difference between the composite and disk GEs is smaller at high heat generation rates.

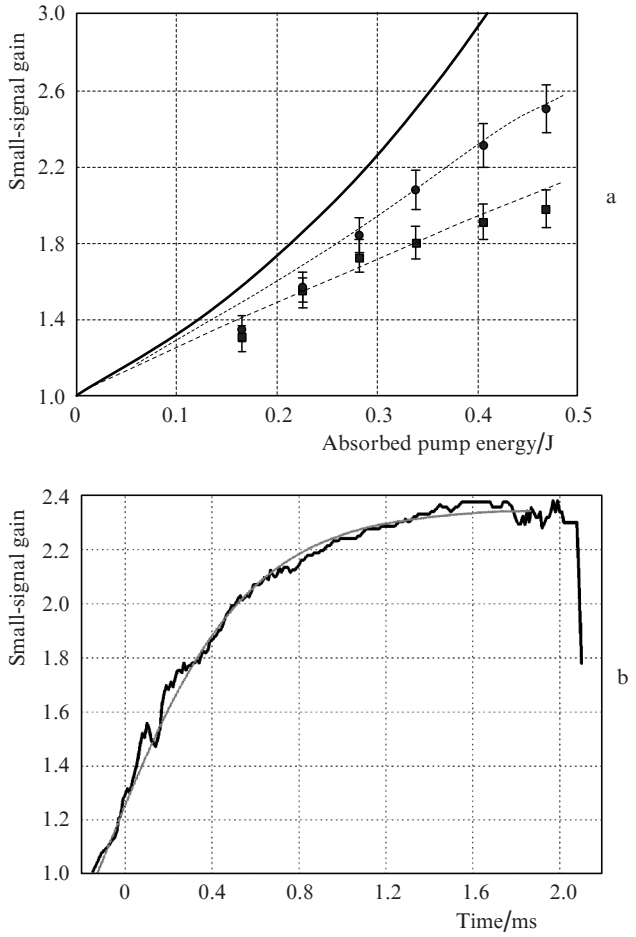

Figure 4. (a) Small-signal gain as a function of absorbed pump energy for a disk GE (■) and composite GE (●). The solid line represents simulation results for a disk with no allowance for ASE. (b) Time dependence of the small-signal gain for a composite GE at an absorbed energy of 0.388 J. The black line shows experimental data and the grey line shows calculation results.

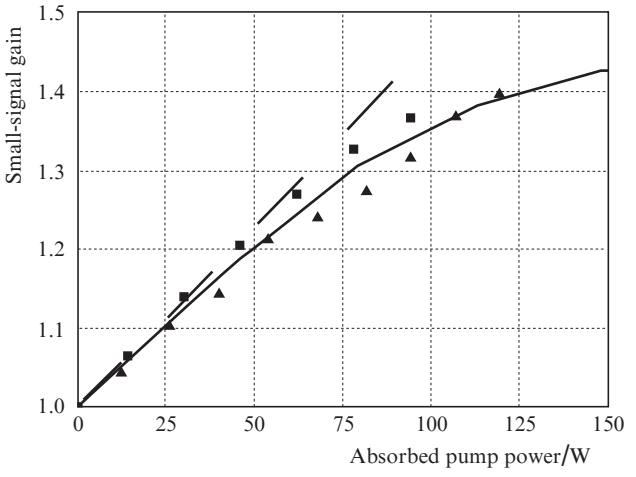

Figure 5. Small-signal gain as a function of absorbed cw pump power for a disk (▲) and a composite GE (■). The lines represent numerical simulation results.

4. Conclusions

We have constructed a theoretical model for the population inversion in Yb:YAG disk GEs and designed a program code for solving a system of balance equations and a nonlinear heat equation with allowance for amplified spontaneous emission, temperature-dependent GE parameters and the population distribution over the energy sublevels of the ytterbium ion. This allows a numerical model to be used in a wide temperature range (80 to 400 K) and for a highly nonuniform heat generation in GEs.

Several features of amplification in disk GEs are worth noting. Intense transverse ASE and parasitic lasing significantly limit the energy stored in such GEs. The problem of increasing the stored energy can be partially solved by using composite GEs and by reducing the pump power density. Effective cooling of disk GEs and the associated significant improvement of their thermo-optical characteristics enable operation at higher average powers, leading to a highly nonuniform temperature profile across the GE and, accordingly, influencing the stored energy and gain coefficient. This must be taken into account in gain coefficient and stored energy calculations. In particular, a strong temperature dependence of thermal conductivity leads to a necessity to solve a nonlinear heat equation. The ability to find the three-dimensional ASE intensity markedly improves the accuracy in gain coefficient and stored energy calculations. A highly nonuniform temperature profile across a GE leads to a necessity to take into account temperature-dependent bulk characteristics of the lasing medium.

The present numerical simulation results agree well with rough theoretical estimates for a uniform pump intensity distribution [21]. Also, there is good agreement between simulation results and experimental data, in particular in parasitic lasing threshold estimates. In all cases, the stored energy is severely limited by ASE and parasitic lasing. An important point is that there is good agreement between theoretical predictions and experimental data at high thermal loads, because the temperature difference in a crystal may reach tens of kelvins, which would lead to a highly nonuniform distribution of material characteristics in the bulk of the GE.

We have compared Yb:YAG disk and composite gain elements as to the effect of amplified spontaneous emission on the stored energy under cw and pulsed pumping. The results demonstrate that the use of composite GEs allows one to markedly reduce the negative influence of these effects and store considerably more energy at a given pump power, which is of special importance because of the high cost of diode pumping.

Acknowledgements. This work was supported by the Presidium of the Russian Academy of Sciences (Extreme Light Fields and Their Applications Programme).

References

1. Fan T.Y., Crow T., Hoden B. *Proc. SPIE Int. Soc. Opt. Eng.*, **3381**, 200 (1998).
2. Brown D.C. *Cryogenically-Cooled Solid-State Lasers*. US Patent 6195372, Feb. 27, 2001.
3. Fan T.Y. *IEEE J. Quantum Electron.*, **29**, 1457 (1993).
4. Dong J., Bass M., Mao Y., Deng P., Gan F. *J. Opt. Soc. Am. B*, **20**, 1975 (2003).
5. Brown D.C., Bowman R., Kuper J., Lee K.K., Mendes J. *Appl. Opt.*, **25**, 612 (1986).

6. Tokita S., Kawanaka J., Fujita M., Kawashima T., Izawa Y. *Appl. Phys. B*, **80**, 635 (2005).
7. Ripin D.J., Ochoa J.R., Aggarwal R.L., Fan T.Y. *Opt. Lett.*, **29**, 2154 (2004).
8. Brown D.C. *J. Sel. Top. Quantum Electron.*, **11**, 587 (2005).
9. Antognini A., Schuhmann K., Amaro F.D., Biraben F., Dax A., Giesen A., Graf T., Hänsch T.W., Indelicato P., Julien L., Kao C.-Y., Knowles P.E., Kottman F., Le Bigot E., Liu Y.-W., Ludhova L., Moschüring N., Mulhause F., Nebel T., Nez F., Rabinowitz P., Schwob C., Taqqu D., Pohl R. *IEEE J. Quantum Electron.*, **45** (8), 993 (2009).
10. Kouznetsov D., Bisson J.-F. *J. Opt. Soc. Am. B*, **25** (3), 338 (2008).
11. Kouznetsov D. *Res. Lett. Phys*., **2008**, 717414-1 (2008).
12. Jianli Shang, Xiao Zhu, Guangzhi Zhu, Wei Wang. *Opt. & Laser Technol*., **44**, 1359 (2012).
13. Speiser J. *Laser Phys*., **19** (2), 274 (2009).
14. Xinghua L., Jiangfeng W., Xiang L., Youer J., Wei F., Xuechun L. *Chin. Opt. Lett*., **9** (11), 111401(2011).
15. Albach D. *Amplified Spontaneous Emission and Thermal Management on a High Average-Power Diode Pumped Solid State Laser. The LUCIA Laser System* (Paris: École Polytechnique ParisTech., 2010).
16. Mukhin I., Perevezentsev E., Vyatkin A., Vadimova O., Palashov O., Khazanov E. *Proc. SPIE Int. Soc. Opt. Eng*., **8080**, 80800B1 (2011).
17. Mukhin I.B., Perevezentsev E.A., Palashov O.V., in *Laser Optics-2012 Techn. Program, ThR1-27* (St. Petersburg, 2012).
18. Casagrande O., Deguil-Robin N., Le Garrec B., Bourdet G.L. *IEEE J. Quantum Electron*., **43** (2), 206 (2007).
19. Mukhin I.B., Palashov O., Khazanov E.A., Vyatkin A.G., Perevezentsev E.A. *Kvantovaya Elektron*., **41** (11), 1045 (2011) [*Quantum Electron*., **41** (11), 1045 (2011)].
20. Mukhin I., Palashov O., Khazanov E., Perevezentsev E., Vyatkin A., Vadimova O. *Techn. Dig. ICONO/LAT 2010* (Kazan', 2010) LTuL40.
21. Konings R.J.M., van der Laan R.R., van Genderen A.C.G., van Miltenburg J.C. *Thermoopt. Acta*, **313** (2), 201 (1998).
22. Vinokurov G.N. *Kvantovaya Elektron*., **4** (9), 1974 (1977) [*Sov. J. Quantum Electron*., **7** (9), 1121 (1977)].